*Int. J. Electrochem. Sci.*, 16 **(2021)** Article Number: 211119, doi: 10.20964/2021.11.03

International Journal of
ELECTROCHEMICAL
SCIENCE
www.electrochemsci.org

# Evaluation of the Anticorrosion and Adsorption Properties of Polyethylene Glycol and Polyvinyl Alcohol for Corrosion of Iron in 1.0 M NaCl Solution

*Arej S Al-Gorair[1], H. Hawsawi[2], A. Fawzy[3], M. Sobhi[4], Ahmed Alharbi[3,*], R.S. Abdel Hameed[5], S. Abd El Wanees[6], M. Abdallah[3,7,*]*

[1] Chem. Depart., College of Sci., Princess Nourah bint Abdulrahman Univ., Riyadh, Saudi Arabia
[2] University College of Alwajh, Alwajh, Tabuk Univ., Tabuk, Saudi Arabia
[3] Chem. Depart. Faculty of Applied Sciences, Umm Al-Qura Univ., Makkah, Saudi Arabia
[4] Chem. Depart. Faculty of Science, Tabuk Univ., Tabuk, Saudi Arabia
[5] Depart. of Basic Sciences, Hail Univ., Hail, 1560 Kingdom of Saudi Arabia
[6] Faculty College of Umluj, Umluj, Tabuk Univ., Tabuk, Saudi Arabia
[7] Chem. Depart., Faculty of Sciences, Benha Univ., Baha, Egypt
[*]E-mail: metwally555@yahoo.com, amaharbi@uqu.edu.sa

*Received:* 9 July 2021 / *Accepted:* 30 August 2021 / *Published:* 10 October 2021

The inhibitory vigor of two polymer molecules namely, polyethylene glycol (PEG) and polyvinyl alcohol (PVA) against the corrosion of iron in 1.0 M NaCl was assessed by chemical and electrochemical technologies. All the computed corrosion parameters from all technologies confirm the inhibitory impact of PEG and PVA compounds. The anticorrosion efficiency increased with the concentration of the polymer molecules to reach 93% and 86% at 500-ppm concentration of PEG and PVA, respectively. The potentiodynamic polarization confirms that the two polymer molecules act as mixed inhibitors. The mechanism of the anticorrosion was explicated in terms of the spontaneous adsorption of these molecules on the iron interface according to the negative values of $\Delta G^{o}_{ads}$. The surface morphology was revealed by SEM images and indicated the building of adsorbed film on the iron surface in the presence of PEG and PVA, which leads to the isolation of iron surface from the corroded NaCl solution. The activation and the adsorption thermodynamics parameters was determined and explicated.

**Keywords:** Iron, , Polyethylene glycol, Polyvinyl alcohol, Polarization, Adsorption.

## 1. INTRODUCTION

Iron is one of the most important products of the Saudi Basic Industries Corporation (SABIC), which is the leading iron and steel manufacturer in the KSA country and the Arabian Gulf. Iron is used in many industrial applications such as buildings, bridges, tunnels, agricultural equipment and many importance industries. Unfortunately, iron will corrode when it is placed in sodium chloride solutions.

Therefore, there are many ways to reduce the risk of corrosion and the deterioration of iron and steel in aqueous solutions, the most important of which is the use of corrosion inhibitors [1-6].

From previous studies, we find that most of the inhibitors are organic molecules containing nitrogen, oxygen, sulfur, or two or all of them [7-12], surfactants compounds [13-16], pharmaceutical drug molecules [17-20], polymer molecules [21-25] and other compounds. All these molecules acted as inhibitors by adsorbing them on the surface of the iron or steel [26-27]. The adsorbent layers coat the active sites on the metal, minimize the corrosion action, and thus enhance the effectiveness of the anticorrosion. The adsorption strength based on the chemical structure of the corrosion inhibitor, the kind of metal or alloy used, the pH of the corrosive solution, the temperature, the presence of some hetro atoms in its structure, the existence of electron donating or repelling groups, and capability to form complex [28].

The fundamental purpose of this research is to try to reduce the corrosion rate of iron in 1M NaCl solution by two polymer molecules, namely, polyethylene glycol (PEG) and poly vinyl alcohol (PVA). Three techniques were utilized to determine the anticorrosion efficiency of the investigated two polymer molecules namely, mass loss (ML), potentiodynamic polarization (PDP) and electrochemical impedance spectroscopy (EIS). The impact of temperature and determination the thermodynamics of the activation and adsorption operation was investigated. In addition, the kind of adsorption isotherm was detected and interpreted.

## 2. EXPERIMENTAL

### *2.1. Materials and techniques*

Fresh solutions utilize in this investigation were prepared from Merck or Aldrich chemicals in twice distilled water. The present study was carried out in 1.0 M NaCl solution as a corrosive solution which was prepared by dissolving the appropriate amounts of sodium chloride reagent (Merck) in bidistilled water. Solutions of the examined polysaccharide inhibitors (polyethylene glycol & poly (vinyl alcohol), Aldrich), were prepared using bidistilled water and they used with concentrations (100 - 500 ppm). The experiments were carried out on iron specimens.

PDP and EIS tests were performed on a thermostated PGSTAT30 potentiostat /galvanostat. Before each experiment, iron electrode (working electrode) was prepared as reported [28] and was directly inserted into the 1.0 M NaCl solution and / or required inhibitor quantity at OCP (open circuit potential) which attained after almost 30 min. of insertion. In PDP, the potential was automatically altered within (-200 to + 200 mV vs. OCP) with a scan rate of 2.0 mV/s. In EIS, the frequency range was: 100 kHz to 0.1 Hz, and the amplitude was 4.0 mV (peak to peak) using AC signals at OCP.

ML tests were done in vessels with a temperature-controlled. The iron specimens were cylinder-shaped rods (almost 13 $cm^2$ area). Iron specimens were also prepared for these tests as stated earlier [28].

*2.2. Surface morphology*

Surface morphology of the surfaces of iron specimens was explored prior to and after adding 300 ppm of the designed two polymer using JEOL Scanning Electron Microscope (SEM) model T-200 with a repeat voltage of 10.0 kV. First, the surfaces of the iron specimens were scratched with various emery papers up to a grade 1200 then rinsed with bidistilled water. Before investigation, the tested specimens were inserted in the examined solution for 24 h at 303 K.

*2.3. Determination of anticorrosion efficiency*

The percentage anticorrosion efficiency (% AE) and surface coverage (θ) of the examines PEG and PVC the three techniques (PDP, EIS and ML) measurements was determined using the next equations [29]:

$$\%AE = [1- Y/ Z] 100 \quad (1)$$

$$\theta = [1- Y/ Z] \quad (2)$$

Where Y and Z represents the values of *I*corr. and mass loss in the case of PDP and ML measurements in the existence of PEG and PVC and in the free case of blank 1M NaCl solutions, respectively. In the case of EIS technology the reverse is occurs, Y and Z represents the charge transfer resistances ($R_{ct}$) in the blank 1M NaCl solution and in the existence of the inhibitors (PEG and PVC) solutions, respectively.

*2.4. Polymer molecules*

The two polymeric compounds utilized in this study, polyvinyl alcohol (PVA) and alginic acid (AA), were utilized as received from Sigma-Aldrich. Their chemical structures are shown in Figure 1.

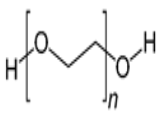


Polyethylene glycol (PEG)


Polyvinyl alcohol (PVA)

**Figure 1.** Chemical structure of PEG and PVA.

## 3. RESULTS AND DISCUSSION

### *3.1. PDP technique*

PDP curves of iron in 1.0 M NaCl-free solution and in the existence of a given concentration of (a) PEG and (b) PVC at 303 K are represented in Fig.2.

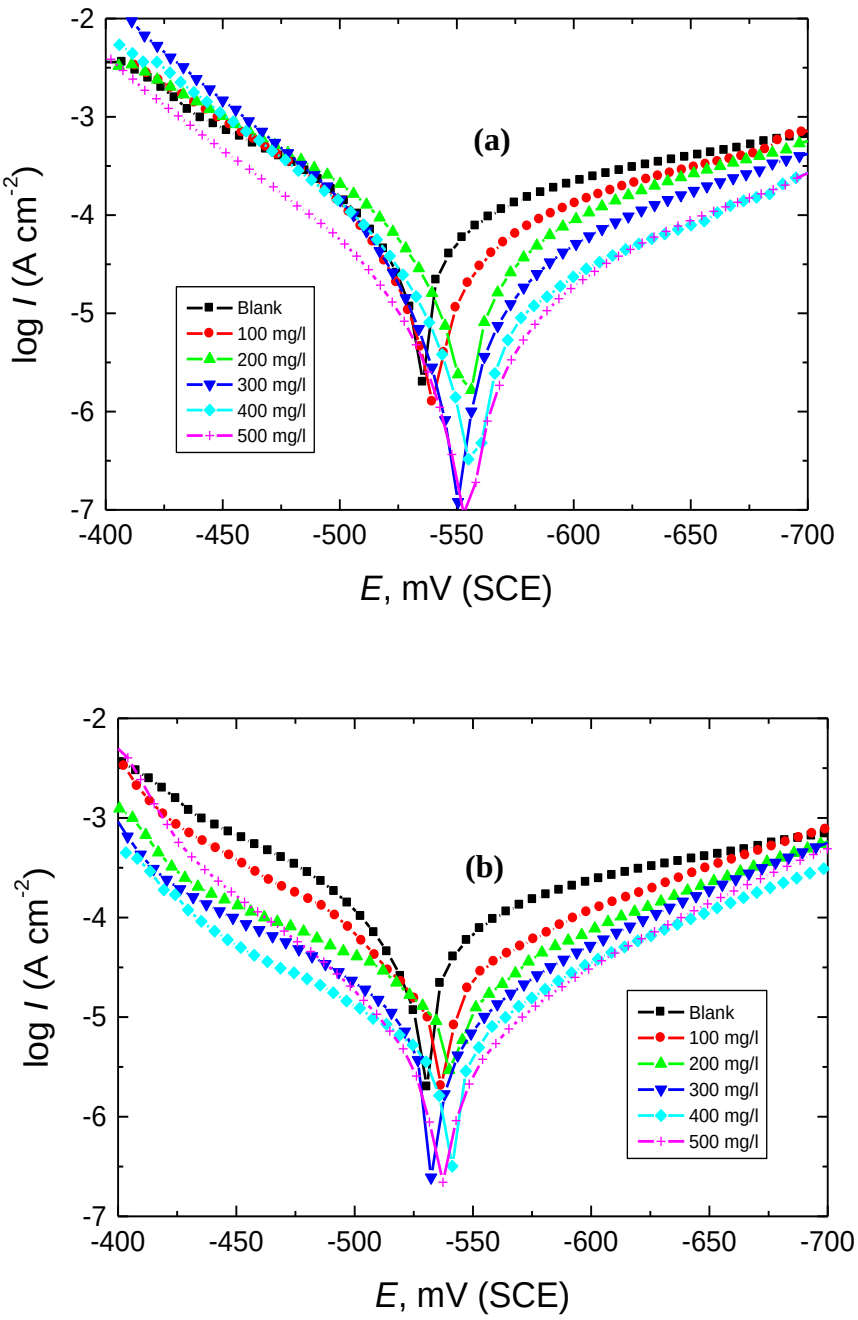


**Figure 2.** PDP curves of iron in 1.0 M NaCl solution in the absence and presence of: (a) PEG and (b) PVC at 303 K.

We note that the general features of these curves, with increasing concentricity of the PEG and PVC, the anodic iron dissolution and cathodic hydrogen evolution are more perspicuous. The cathodic and anodic Tafel lines are moved to more active and nobler potentials with respect to the free curves. The corrosion parameters such as anodic Tafel ($\beta_a$) and cathodic ($\beta_c$) Tafel slopes, corrosion potential ($E_{corr}$), corrosion current density ($I_{corr.}$) and the anticorrosion efficiency (% AE) are collected in Table 1. The values of $\beta_a$ and $\beta_c$ Tafel slopes are nearly constant. The shift in $\beta_a$ and $\beta_c$ around 22 and 24 mV in case of the presence of PEG but in the presence of PVC the shift are equal to 17 and 32 mV. The $E_{corr}$ value are shifted slightly or nearly constant in to the active direction, decreasing from a value of -528 in free NaCl solution to -553 mV and -546 mV(SCE)in case of the addition of 500ppm of PEG and PVC molecules ,respectively. These data demonstrate the PEG and PVC molecules performed as mixed inhibitors **[30, 31].** As the concentricity of polymer molecules elevated, the $I_{corr.}$ values continued reducing and thus the %AE values increased. These outcomes indicate the anticorrosion impact of the PEG and PVC molecules. At all the concentricity of the two inhibitors, %AE of PEG is more efficient than for PVC. This behavior illustrated at the end of the manuscript.

**Table 1.** PDP data for the corrosion of iron in free1.0 M NaCl solution and with certain concentrations of PEG and PVA molecules at 303 K.

| **Inh.** | **Inh. Concn. (mg/l)** | **$-E_{corr}$ (mV(SCE))** | **$\beta_a$ (mV/dec.)** | **$-\beta_c$ (mV/dec.)** | **$I_{corr}$ (µA/cm$^2$)** | **%AE** | **θ** |
|---|---|---|---|---|---|---|---|
| | **0** | **528** | **82** | **124** | **51.96** | -- | -- |
| **PEG** | **100** | 533 | 79 | 118 | 28.11 | 46 | 0.46 |
| | **200** | 555 | 72 | 113 | 18.20 | 65 | 0.65 |
| | **300** | 551 | 66 | 106 | 9.89 | 81 | 0.81 |
| | **400** | 554 | 62 | 102 | 6.75 | 87 | 0.87 |
| | **500** | 553 | 60 | 98 | 4.16 | 92 | 0.92 |
| **PVA** | **100** | 532 | 76 | 118 | 27.53 | 47 | 0.47 |
| | **200** | 536 | 78 | 108 | 18.73 | 64 | 0.64 |
| | **300** | 538 | 68 | 103 | 10.90 | 79 | 0.79 |
| | **400** | 540 | 70 | 98 | 8.83 | 83 | 0.46 |
| | **500** | 546 | 65 | 92 | 7.78 | 85 | 0.65 |

*3.2. EIS measurement*

Impedance diagram (Fig. 3a) presented in a complex plane, describing the behavior of iron in NaCl solution without and with certain concentrations of PEG and PVA compounds. As shown from this diagram, the single depressed capacitive imperfect semicircles were usually displayed due to the roughness of the teste surface, the dispersion of frequency and the heterogeneity of the tested samples [32]. Also, the similarities between these plots in both the blank and that of tested solutions with additive pointing to the tested iron samples perform a corrosion reaction which are under charge transfer control,

and this type of additives not alter the mechanism. In addition, it can be shown from a Fig. that the semicircles diameters in case of additive are longer than others and this pointing to the inhibiting effect of these compounds by blocking the active sites on the iron surface and hence achieve protection [33].

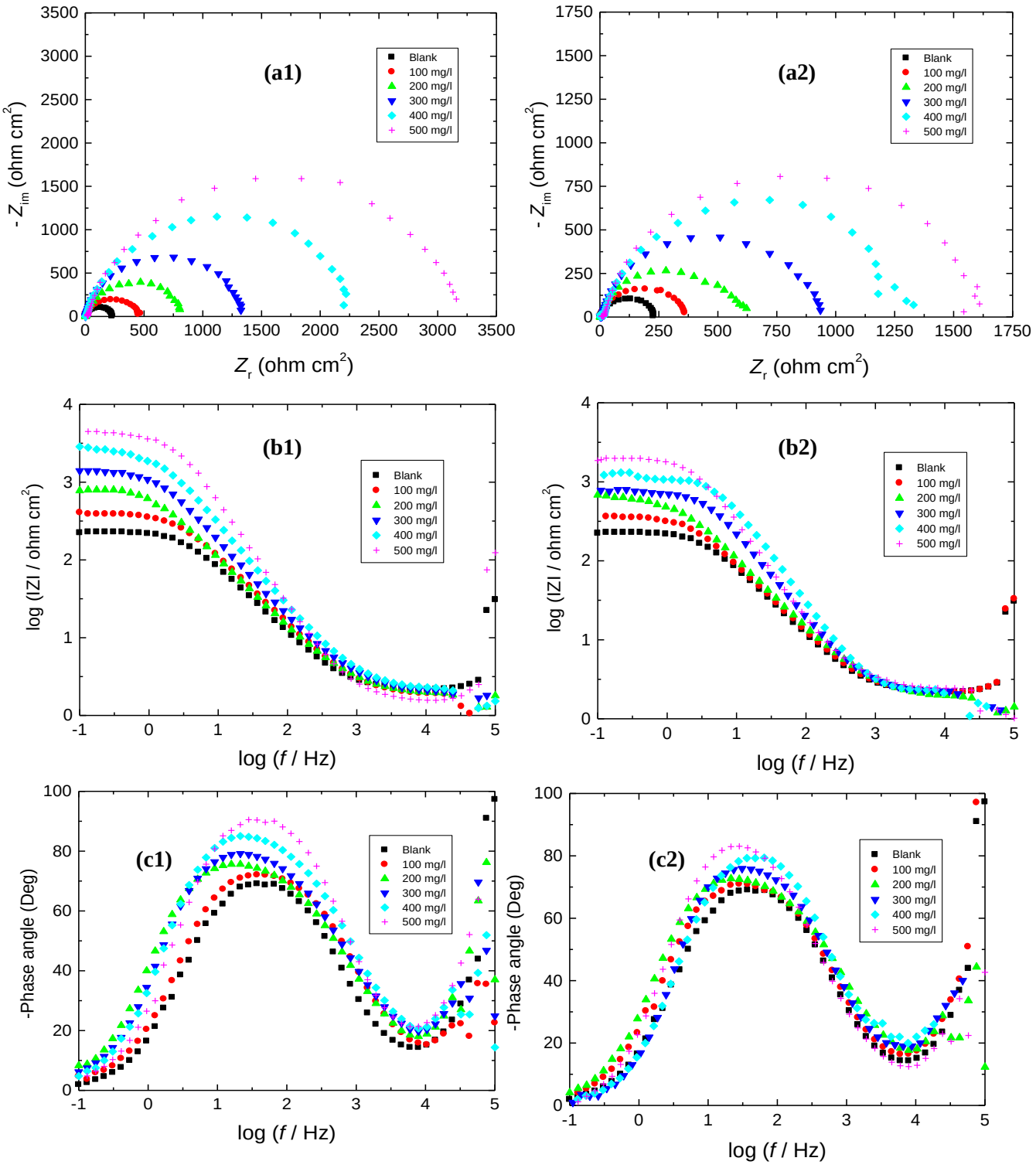


**Figure 3.** (a) Nyquist, (b) Bode magnitude plot, and (c) Bode phase plot for the corrosion of iron in free 1.0 M NaCl solution at 303 K and with some concentrations of: (1) PEG and (2) PVA

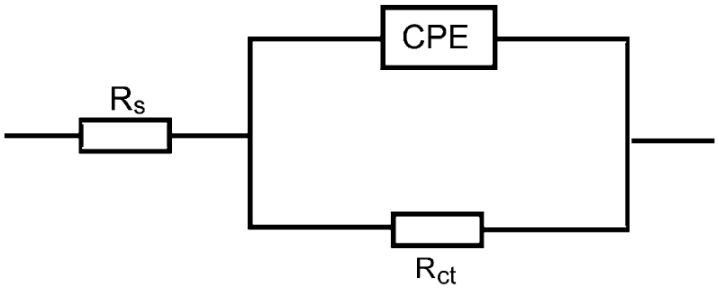


**Figure 4.** Electrochemical equivalent circuit applied to fit the EIS parameters for the corrosion of iron in 1.0 M NaCl solution in the absence and presence of the tested polymers.

**Table 2.** EIS data for the corrosion of iron in 1.0 M NaCl solution in the absence and presence of polyethylene glycol (PEG) and poly (vinyl alcohol) (PVA) at 303 K.

| **Inhibitor** | **Inhibitor Concn. (mg/l)** | ***R*s (ohm cm$^2$)** | ***R*ct (ohm cm$^2$)** | **CPE (µF/cm$^2$)** | **%AE** |
|---|---|---|---|---|---|
| | **0** | **2.04** | **225** | **707** | **--** |
| **PEG** | **100** | 1.17 | 461 | 384 | 51.19 |
| | **200** | 1.52 | 805 | 248 | 72.05 |
| | **300** | 2.65 | 1324 | 172 | 83.01 |
| | **400** | 11.21 | 2245 | 118 | 89.98 |
| | **500** | 19.61 | 3216 | 99 | 93.00 |
| **PVA** | **100** | 1.81 | 382 | 463 | 41.09 |
| | **200** | 1.37 | 608 | 327 | 62.99 |
| | **300** | 3.03 | 938 | 242 | 76.01 |
| | **400** | 3.98 | 1327 | 197 | 83.04 |
| | **500** | 9.25 | 1608 | 186 | 86.01 |

The equivalent circuit that fit these plots were Randles equivalent circuit ($R_s$ ($R_{ct}$/CPE). Fig. 5. where , Rs is the solution resistance, $R_{ct}$ is the charge transfer resistance related to the OCP corrosion reaction, while the CPE represents a constant phase element related to the non-ideal capacity ($C_{dl}$). The CPE is introduced as follows [34]:

$$Z_{CPE} = \frac{1}{Y_o(jw)^n} \qquad (3)$$

Where $Y_0$ is a CPE constant, j is the imaginary number, ω is the angular frequency (ω = 2πf, f represents the AC frequency in Hz), n is a phase shift, which is related to the system homogeneity, when the CPE display a pure capacitance, n = 1. The electrical double layer capacitance ($C_{dl}$) was calculated by the following equation [35]:

$$C_{dl} = Y_o\,(\mathrm{w\,max})^{n-1} \qquad (4)$$

The EIS parameters obtained from the tested samples were investigated in Table 2. As seen from this table, the increase in $R_{ct}$ with the additive concentration, also the decrease in $C_{dl}$ pointing to the inhibiting effect of these additives. The anticorrosion efficiency (IE %) was calculated using equation 1.

The decrease of the $C_{dl}$ value reflects an increase in the double layer thickness (d), which indicates the possibility of formation of protective film on the iron surface by adsorption [35].

$$C_{dl} = \frac{\varepsilon^{o} x \varepsilon}{d} S \qquad (5)$$

The thickness of the adsorbed film is denoted by d, the air permittivity ε° and that of the medium ε (dielectric constant) and S is the tested electrode surface area.

Further, the Bode and phase angle plots are given in Fig. 3b and 3C, which aids to give valuable information about the corrosion process. As seen, the impedance modulus, have an increase with the increase of the investigated compounds at low frequencies, which pointing to the adsorption of these compounds in the metal surface and hence, inhibiting the corrosive effect NaCl solution [36]. In addition, it is clearly shown the presence of a single peak in the phase angle plots that confirms the existence of a single time constant at the metal/ solution interface.

### *3.3. ML measurements*

Fig.5 displays show the ML-immersion time curves for iron in free 1.0 M NaCl solution and contains certain concentrations of (a) PEG and (b) PVC. The corrosion rate (CR) was determined from this equation:

$$CR = ML_o / At \qquad (6)$$

Where: A: is the area of electrode in $cm^2$, t is the immersion time in h, $ML_o$ is the difference in mass loss of iron before and after exposure to the corrosive solutions

The commonalty features of this figure reveals that by augmentation the concentricity of polymer molecules the ML reduced, the values of CR increases, the values of **θ** and the %AE increases .This demonstrates that the PEG and PVC diminishes the corrosion of iron or act as an inhibitors. At all the studied concentrations the % AE of PVC more than PEC.

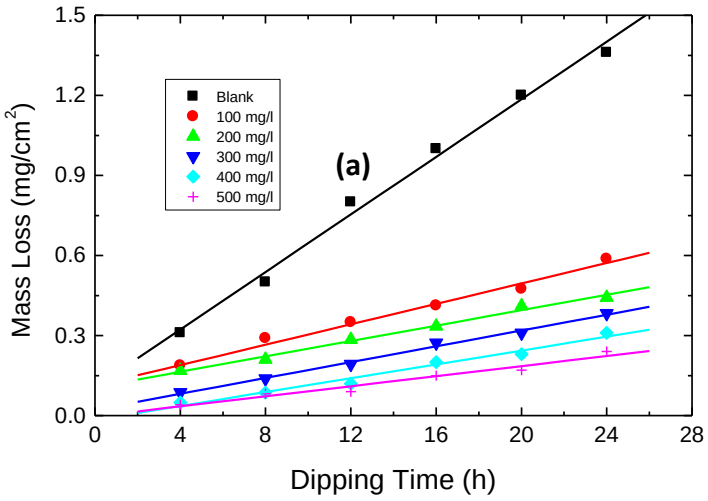

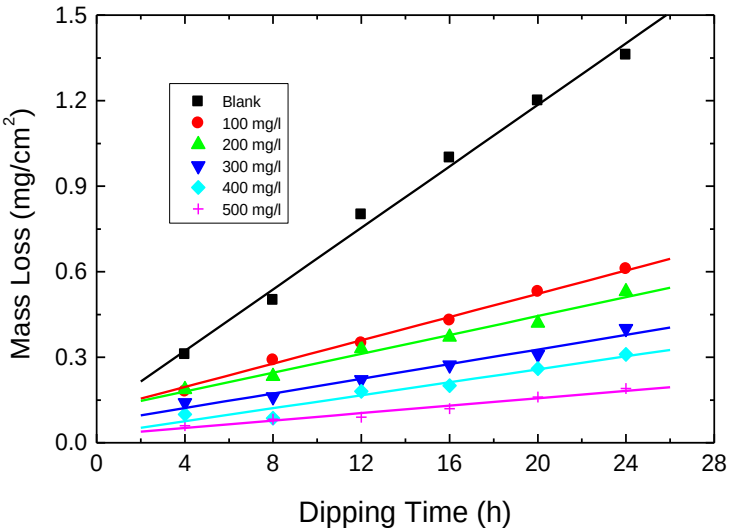


**Figure 5.** Plots of ML versus immersion time for the dissolution of iron in blank 1.0 M NaCl solution and with certain concentrations of: (a) PEG and (b) PVC at 303 K.

*3.4. Activation Kinetic Parameters*

The influence of high temperature on the ML of iron in a free 1.0 M NaCl solution with some concentrations ranging from 100 to 500 mgl$^{-1}$ of PEG and PVC molecules was studied. The acquired corrosion data such as CR, % AE and Θ at different temperatures are recorded in Table 3. It is apparent that, as the temperature increases the CR increases while the the values of Θ and the % AE decreases. This elucidates that increasing the temperature reduced the adsorption of the two polymer molecules and subsequently accelerated the dissolution process and this demonstrate that the adsorption of PEG and PVC on the surface of the iron is physical [37].

**Table 3.** Average values of CR of iron in free 1.0 M NaCl solution and with certain concentrations of PEG and PVC at different temperatures.

| **Inhibitor** | **Inhibitor Concn. (mg/l)** | **Temperature (K)** | | | | | | | | | | | |
|---|---|---|---|---|---|---|---|---|---|---|---|---|---|
| | | **293** | | | **303** | | | **313** | | | **323** | | |
| | | **CR** | **% AE** | **θ** | **CR** | **% AE** | **θ** | **CR** | **% AE** | **θ** | **CR** | **% AE** | **θ** |
| | **0** | **24.98** | -- | -- | **31.03** | -- | -- | **35.01** | -- | -- | **41.91** | -- | -- |
| **PEG** | **100** | 10.25 | 59 | 0.59 | 13.95 | 55 | 0.55 | 16.10 | 54 | 0.54 | 21.42 | 49 | 0.49 |
| | **200** | 7.01 | 72 | 0.72 | 9.30 | 70 | 0.70 | 11.55 | 67 | 0.67 | 15.12 | 64 | 0.64 |
| | **300** | 4.75 | 81 | 0.81 | 5.89 | 81 | 0.81 | 8.42 | 76 | 0.76 | 12.18 | 71 | 0.71 |
| | **400** | 3.02 | 88 | 0.88 | 4.96 | 84 | 0.84 | 6.65 | 81 | 0.81 | 9.26 | 78 | 0.78 |
| | **500** | 2.01 | 92 | 0.92 | 3.41 | 89 | 0.89 | 4.55 | 87 | 0.87 | 8.39 | 80 | 0.80 |

| | | | | | | | | | | | | | |
|---|---|---|---|---|---|---|---|---|---|---|---|---|---|
| **PVA** | **100** | 11.50 | 54 | 0.54 | 14.88 | 52 | 0.52 | 18.55 | 47 | 0.47 | 24.71 | 41 | 0.41 |
| | **200** | 7.51 | 70 | 0.70 | 10.54 | 66 | 0.66 | 13.65 | 61 | 0.61 | 18.04 | 57 | 0.57 |
| | **300** | 5.75 | 77 | 0.77 | 8.06 | 74 | 0.74 | 9.83 | 72 | 0.72 | 14.63 | 65 | 0.65 |
| | **400** | 4.26 | 83 | 0.83 | 6.20 | 80 | 0.80 | 7.35 | 79 | 0.79 | 10.46 | 75 | 0.75 |
| | **500** | 3.52 | 86 | 0.86 | 5.89 | 81 | 0.81 | 6.31 | 82 | 0.82 | 10.05 | 76 | 0.76 |

Activation parameters such as activation energy (Ea*), enthalpy of activation (ΔH*) and activation entropy (ΔS*) for dissolving iron in 1.0 M free NaCl solution and at certain concentrations of PEG and PVC were determined from Arrhenius and transition state equations [38, 39]

$$\text{Ln CR}=\ln A - \frac{E_a^*}{RT} \quad (7)$$

$$\ln\left(\frac{CR}{T}\right)=\left(\ln\frac{R}{Nh}+\frac{\Delta S^*}{R}\right)-\frac{\Delta H^*}{R}\frac{1}{T} \quad (8)$$

Where, A is the frequency factor, N is Avogadro's number, h is the Planck's constant and R is the gas constant.

Figure 6. represents the Arrhenius diagrams (ln CR vs 1/T) for the dissolution of iron in 1.0 M NaCl solution alone and with different concentrations of (a) PEG, and (b) PVC. A linear plot was obtained with linear regression ($R^2$) close to one illustrating the dissolution of iron in 1.0 M NaCl solution can be clarified using the kinetic model. $E_a$* values were determined from the slope of the Arrhenius plots and recorded in Table 4. The values of $E_a$*in the occurrence of PEG and PVC compounds are more than the blank1.0 M NaCl and can be elucidated as due to physical adsorption [40] . Higher $E_a$* resulted in lower CR due to the creation of film on the iron surface serving as an energy barrier for iron corrosion [41].

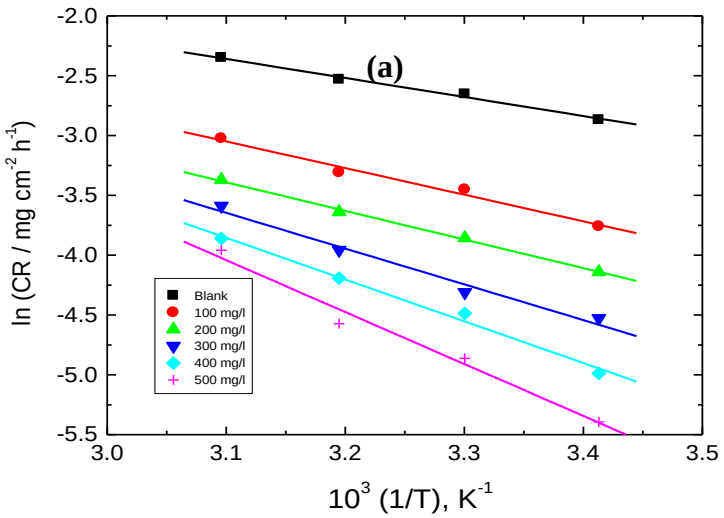

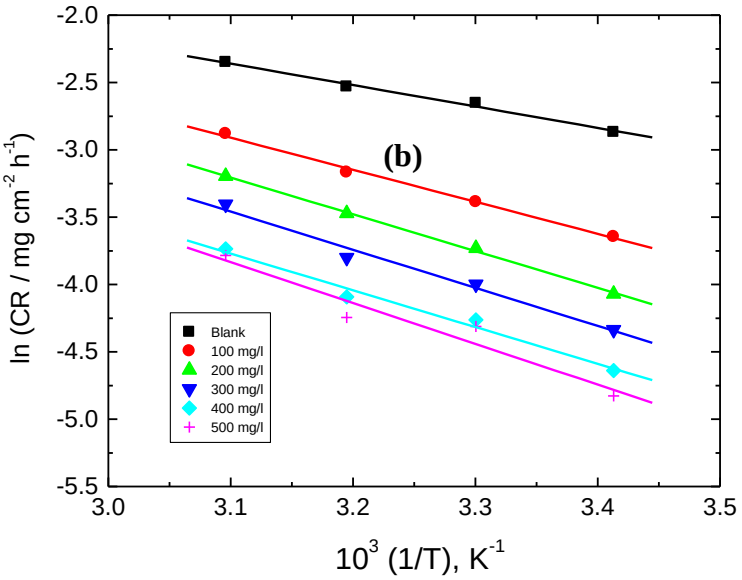


**Figure 6.** Arrhenius plots for the corrosion of iron in 1.0 M NaCl solution alone and with different concentrations of (a) PEG, and (b) PVC.

Fig .7 displays the Transition state plots ln (CR/ T) vs. 1/ T for dissolving iron in 1.0 M free NaCl solution and with some concentrations of PEG and PVC molecules. A straight line was obtained with slope equal to $\Delta H^*$ / 2.303 R and the intercepts equal to log R/Nh + $\Delta S^*$ / 2.303R , The values of $\Delta H^*$ and $\Delta S^*$ are determined and recorded in Table 4 The positive values of $\Delta H^*$ reveals the endothermic behavior of PEG and PVC on the iron surface. This behavior can be explained by the existence of an energy barrier for the corrosion process due to the presence of these polymer compounds, that is, the adsorption process shows a higher enthalpy of the corrosion process. The negative values of $\Delta S^*$ confirm the good adsorption of PEG and PVC on the iron surface. This demonstrates that the activated compound in the rate-limiting step is an association rather than disengagement step, which means that the minimize the disordering occurs on the transition from the reactants to the activated compound [42].

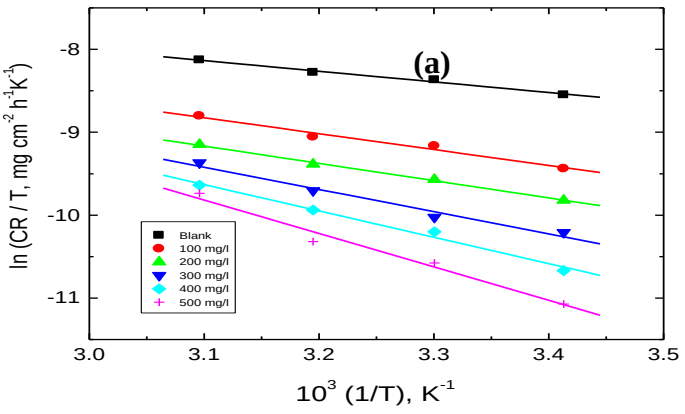

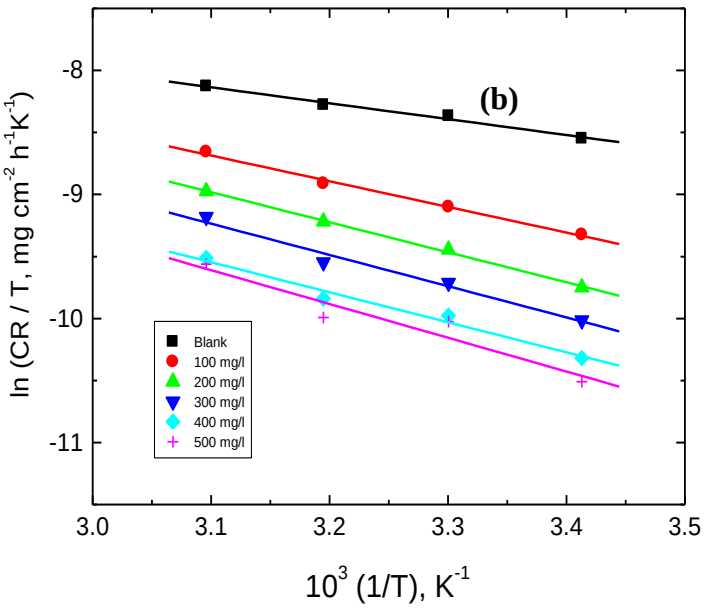


**Figure 7.** Transition state plots for the corrosion of iron in 1.0 M NaCl solution alone and with different concentrations of (a) PEG, and (b) PVC.

**Table 4.** Activation parameters plots for iron in the blank 1.0 M NaCl solution and with of certain concentrations of PEG and PVA.

| **Inhibitor** | **Inhibitors Concn. (mg/l)** | $E_a^*$ **kJ mol$^{-1}$** | $\Delta H^*$ **kJ mol$^{-1}$** | $\Delta S^*$ **J mol$^{-1}$ K$^{-1}$** |
|---|---|---|---|---|
| | **0** | 13.14 | 10.64 | -34.92 |
| **PEG** | **100** | 18.54 | 15.96 | -24.11 |
| | **200** | 19.87 | 17.29 | -22.45 |
| | **300** | 24.86 | 22.19 | -9.98 |
| | **400** | 29.06 | 26.44 | -1.83 |
| | **500** | 35.99 | 33.42 | -22.45 |
| **PVA** | **100** | 19.75 | 17.13 | -19.12 |
| | **200** | 22.66 | 20.12 | -12.48 |
| | **300** | 23.47 | 20.95 | -11.64 |
| | **400** | 22.70 | 20.24 | -16.63 |
| | **500** | 25.19 | 22.61 | -9.97 |

*3.5. Surface morphology*

Fig.8. displays SEM micrographs of iron surface; (a) before immersion, (b) after immersion in 1.0 M NaCl solution for 24 h, (c, d) after 24 h immersion in 1.0 M NaCl with 300 ppm of PEG and PVA, respectively, at 303 K. It is obvious that the surface of iron is smooth before being exposed to the corrosive medium (Fig.8a). When the iron surface is immersed in the 1.0 M NaCl corrosive solution. The surface appeared corrosive by appearance of some etched grain boundaries (Fig.8b). This demonstrate that the iron surface is corroded in the presence of 1.0 M NaCl. The corrosive surface was improved upon addition of 300 ppm of PEG and PVA after one day immersion in 1.0 M NaCl, at 303 K (Fig.8 c and d) , respectively. PEG and PVA form an adsorbed film on the surface of iron. This film is more pronounced in the case of PVA, which confirms higher anticorrosion efficiency of PVA compared to PEG

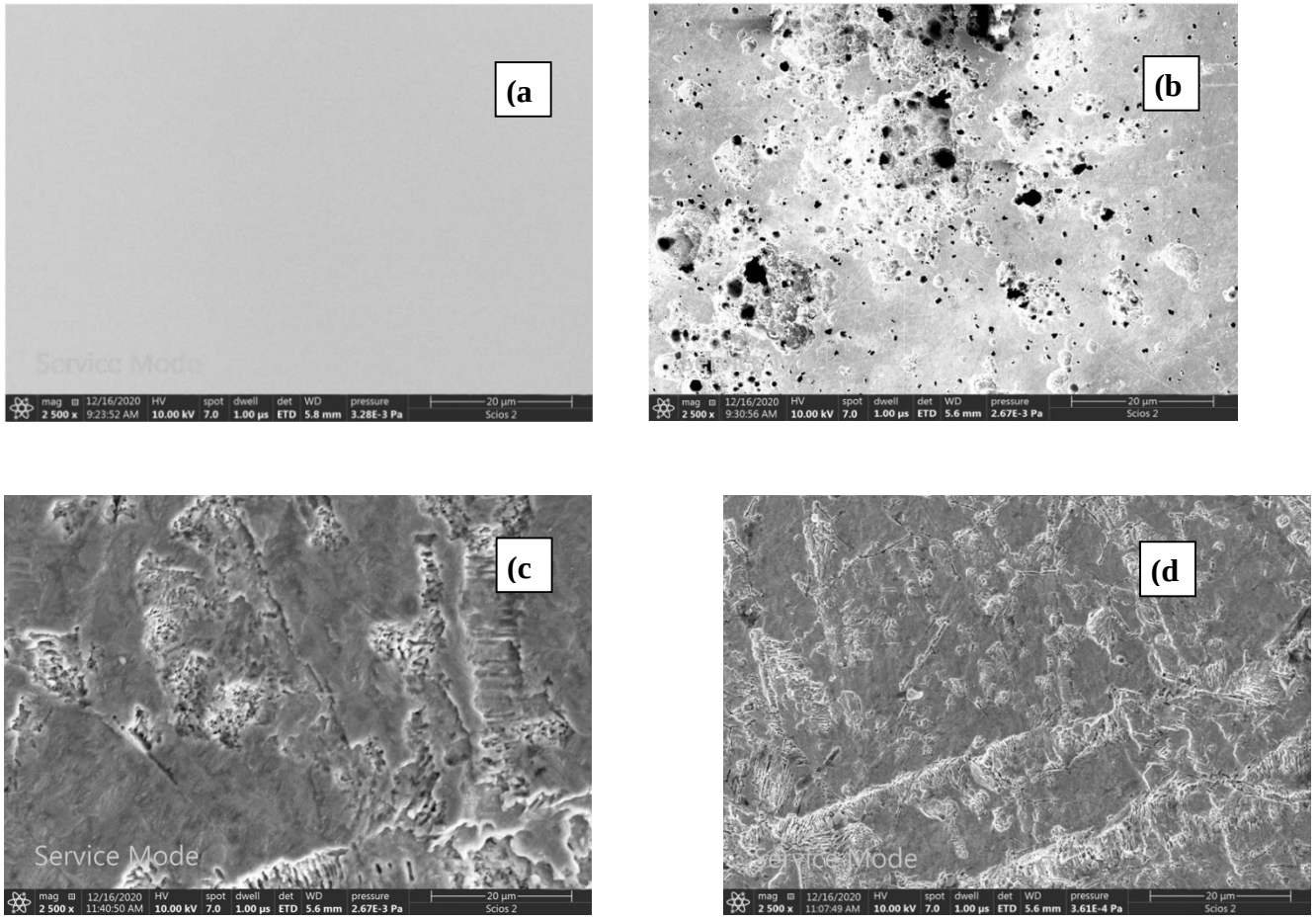


**Figure 10.** SEM micrographs of iron surface; (a) before immersion, (b) after immersion in 1.0 M NaCl solution for 24 h, (c, d) after one day immersion in 1.0 M NaCl with 300 ppm of PEG and PVA, respectively, at 303 K.

*3.6. Adsorption considerations*

The anticorrosion activity of the polymer molecules on the corrosion of iron in 1.0 M NaCl solution based mainly on the replacement operation between polymer molecules in aqueous phase ($P_{(aqu)}$) and number the water molecule adsorbed on the iron surface according to the next equation:

$$P_{(aqu)} + \alpha H_2O_{(sur)} \longrightarrow P_{(sur)} + \alpha H_2O_{(aq)} \quad (9)$$

Where, α is defined as the size ratio and simply equals the number of water adsorbed molecules that have been subrogated by one polymer molecule. The adsorption depends on the chemical composition the polymer used, the type of iron used, the concentration of corrosive medium, temperature and the $p^H$ of the solution.

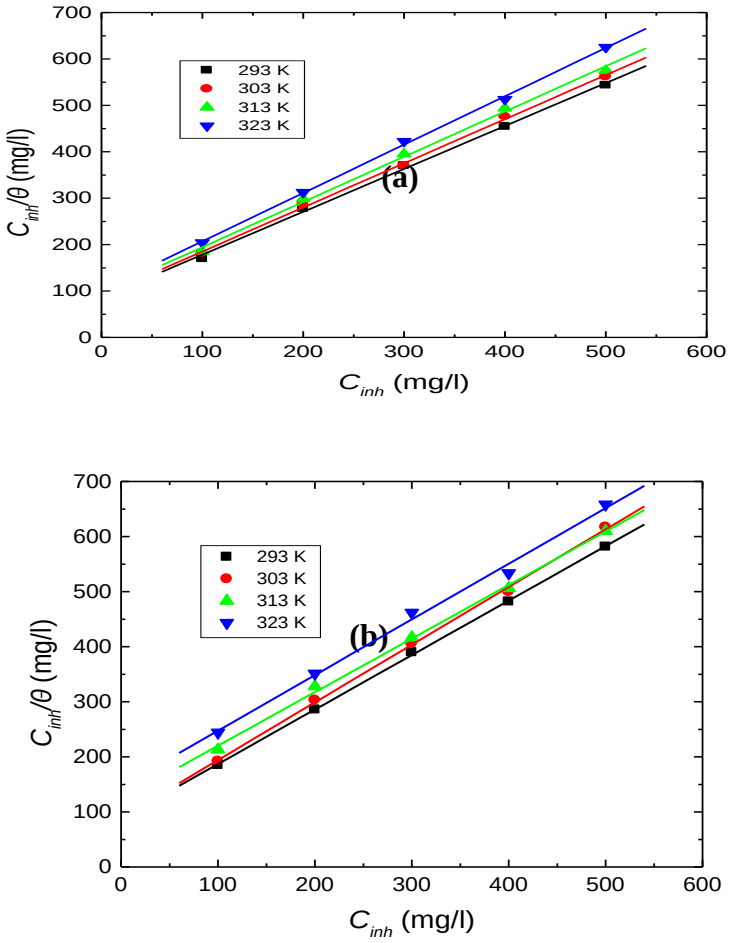


**Figure 8.** Langmuir isotherms for: (a) PEG, and (b) PVA adsorbed on iron surface in 1.0 M NaCl solution at various temperatures.

Also, the adsorption provides knowledge on the interaction between the adsorbed polymer molecules themselves as well as their interaction with the iron surface. To arrive at a suitable isotherm,

the value of θ is entered into the different isotherms and the preferred isotherm is chosen. We find the adsorption of the polymer molecules follows the Langmuir isotherm by applying the next equation [43]:

$$\frac{C_{inh}}{\theta} = \frac{1}{K_{ads}} + C_{inh} \qquad (10)$$

where $K_{ads}$ is the equilibrium constant of adsorption process.

Fig.8 (a &b) represent the Langmuir plots ($C_{inh}$ / θ versus $C_{inh}$) of the adsorption of PEG and PVA on the iron surface at certain temperatures ranging between 293 to 323K. Straight lines were acquired with slope nearly equal (1±0.09). This isotherm refers to a single adsorbed layer of polymer molecules on the surface of iron and zero interaction between the adsorbed species. From the intercept of Langmuir plots we determine the values of $K_{ads}$ and registered in Table 5.

The values of $K_{ads}$. decreases with rising temperatures. The values of the free energy of the adsorption was calculated from the next equation [43]:

$$\Delta G^{o}_{ads} = -RT\ln(55.5K_{ads}) \qquad (11)$$

Where the value of 55.5 is the concentration of water in mol $l^{-1}$.

The values of $\Delta G^{o}_{ads}$ are listed in Table 5. In the case of PEG the values of $\Delta G^{o}_{ads}$ ranged from - 25.09 kJ, $mol^{-1}$ to -27.20 kJ $mol^{-1}$ but in case of PVA it is ranged between -25.03 kJ $mol^{-1}$ and-26.23 kJ $mol^{-1}$.The negative values of $\Delta G^{o}_{ads}$ demonstrates the spontaneous adsorption of PEG and PVA on the iron surface. From the values of $\Delta G^{o}_{ads}$ confirm the adsorption the two polymer molecules are physical adsorption.

The enthalpy of adsorption can be determined from the van't Hoff equation, [44]

$$\ln K_{ads} = \frac{-\Delta H^{o}_{ads}}{RT} + \text{Constant} \qquad (12)$$

Fig.10. displays the Van't Hoff plots for PEG and PVA adsorbed on iron surface in 1.0 M NaCl solution. Straight lines were obtained.

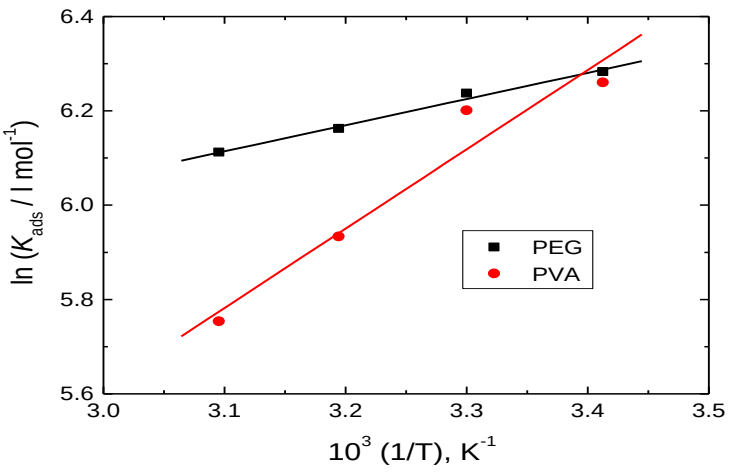


**Figure 10.** Van't Hoff plots for PEG and PVA adsorbed on iron surface in 1.0 M NaCl solution.

The values of $\Delta H^{o}_{ads}$ were determined from the slope of the straight lines and recorded in Table 5. The negative values of $\Delta H^{o}_{ads}$ confirm the adsorption of PEG and PVA on the iron surface are exothermic. The entropy of the adsorption can be determined by applying the Gibbs–Helmholtz equation [44]:

$$T\Delta S^{o}_{ads} = \Delta H^{o}_{ads} - \Delta G^{o}_{ads} \quad (13)$$

The determined values of $\Delta S^{o}_{ads}$ are recorded in Table 5. The positive sign of $\Delta S^{o}_{ads}$ demonstrates the increase in heterogeneity on the iron interface/solution during adsorption of PEG and PVC on the iron surface.

**Table 5.** Thermodynamic adsorption parameters for the corrosion of iron in free 1.0 M NaCl and with presence of PEG and PVA at certain temperatures.

| **Inhibitor** | **Temp. (K)** | **$10^{-2}$ $K_{ads}$ l mol$^{-1}$** | **$\Delta G^{o}_{ads}$ kJ mol$^{-1}$** | **$\Delta H^{o}_{ads}$ kJ mol$^{-1}$** | **$\Delta S^{o}_{ads}$ J mol$^{-1}$ K$^{-1}$** |
|---|---|---|---|---|---|
| **PEG** | **293** | 5.35 | -25.09 | -4.61 | 69.89 |
| | **303** | 5.11 | -25.83 | | 70.03 |
| | **313** | 4.74 | -26.48 | | 69.89 |
| | **323** | 4.51 | -27.20 | | 69.93 |
| **PVA** | **293** | 5.23 | -25.03 | -13.97 | 37.75 |
| | **303** | 5.14 | -25.84 | | 39.18 |
| | **313** | 3.77 | -25.89 | | 38.08 |
| | **323** | 3.15 | -26.23 | | 37.97 |

*3.7. Mechanism of anticorrosion*

The inhibitory strength of PEG and PVA molecules on the corrosion of iron in 1.0 M NaCl solutions was assessed by chemical and electrochemical techniques.. It is evident that the % AE determined from all the applied techniques depends on the concentration of the corrosive solution, the nature of iron used, the type of adsorption and surface environments. All corrosion parameters confirmed the anticorrosion impact of the two polymer molecules. Fig 11(a& b) represents the relationship between the % AE computed from all three technologies and concentration of PEG (Fig 11 a) and PVA (Fig.11b). It is evident that the % AE increases with increasing polymer concentrations. The sequence of % AE acquired from all measurements that are compatible with slight difference in the % AE. This is due the difference of experimental condition. This validates these tools in the measurements of the inhibitors examined.

These outcomes indicated that the inhibitory impact of the PEG and PVA molecules arises from the spontaneous adsorption of these molecules on the iron interface according to the negative values of

ΔGoads .The anticorrosion efficiency depends on several factors such as the chemical structure, the molar mass of polymer molecules, the nature of the interaction between the iron and polymer molecules , the capability to form complex and other factors. It is obvious that the PEG and PVA molecules are more efficient inhibitor than polyethylenemine [45], poloxamer, pectin [22], maltodextrin and chitosan[25] and poly aspartic acid/chitosan complex [46]. The sequence of % AE from all techniques utilized demonstrates that the % AE of PEG is more than PVA due to the higher molar mass of PEG .This led to more coverage area of the surface by inhibitor and more adsorbed film formed on the surface of iron.

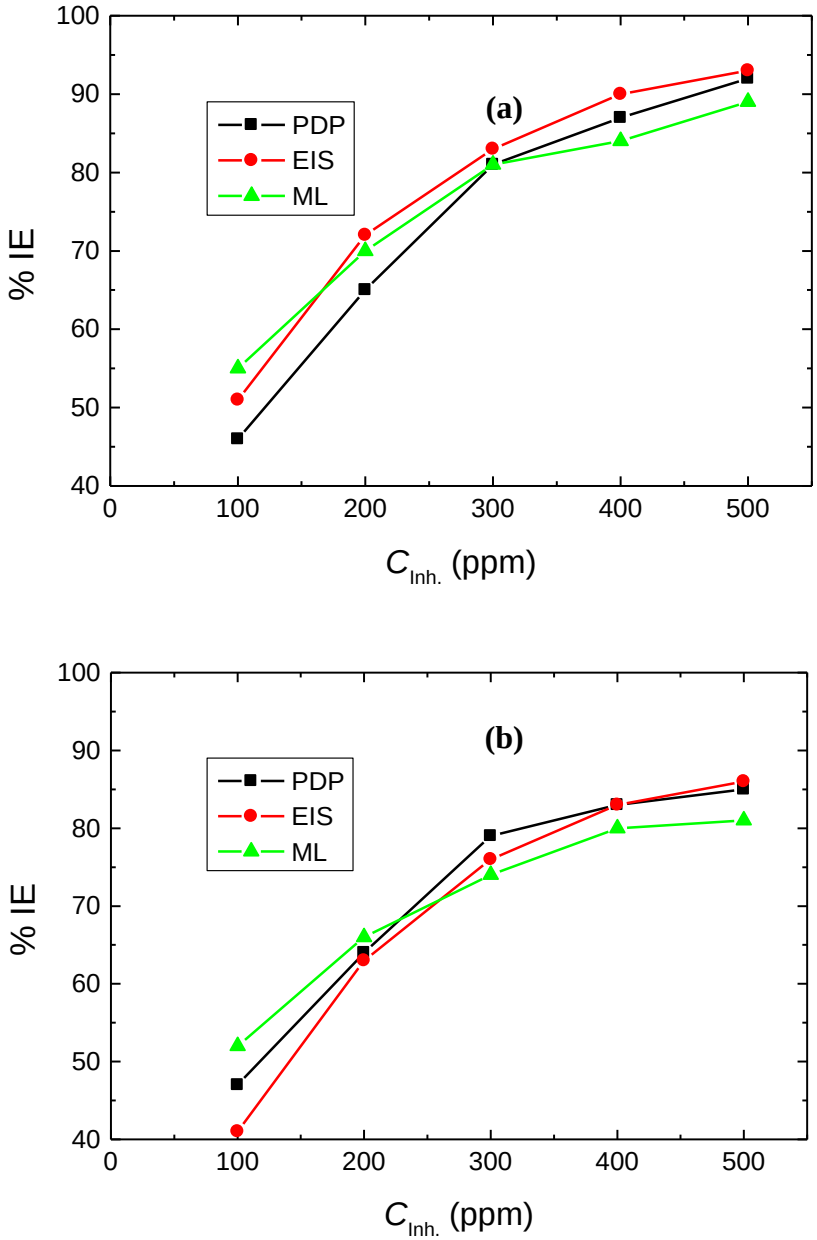


**Figure 11.** Variation of the % AE: (a) PEG and (b) PVA with their concentrations in the corrosion of iron in 1.0 M NaCl solution at 303 K using the different employed techniques.

## 4. CONCLUSIONS

1. PEG and PVA act as a good inhibitor for the corrosion of iron in1.0 M NaCl solution.
2. Polarization measurements confirmed that PEG and PVA are a mixed inhibitor
3. The inhibitory impact of PEG and PVA is attributed to their spontaneous adsorption on the iron Surface
4. Adsorption of PEG and PVA on the iron surface follows the Langmuir isotherm
5. SEM surface morphology images showed that the formation of an adsorbed layer on iron surface
6. %AE of PEG is more than PVA owing to the higher molar mass of it
7. The %AE obtained from the employed techniques is almost consistent with each other

ACKNOWLEDGMENT
The authors would like to thank the Deanship of Scientific Research at Umm Al-Qura University for the continuous support. This work was supported financially by the Deanship of Scientific Research at Umm Al-Qura University (Grant Code:19-SCI-1-01-0039).

## References

1. A. Fawzy, M. Abdallah, Alfakeer, H. M. Ali., *Int. J. Electrochem. Sci.,* 14 (2019) 2063.
2. M. Abdallah, A. Fawzy, A. Al Bahir, *Int. J. Electrochem. Sci.*, 15 (2020) 4739.
3. M. Abdallah, A. Al Bahir, H. M. Altass, A. Fawzy, N. El Guesmi, Arej S Al-Gorair, F. Benita, , I. Wards, A. Zarrouk, *J .Mol. Liq.*, 330, ( 2021) 115702.
4. M. Abdallah K.A. Soliman, Arej S Al-Gorair, A. Al Bahir, Jabir H. Al-Fahemi, M.S. Mattawa, Salih S. Al-Juaid, RSC *Adv.*,11 (2021)17092.
5. M. Abdallah, I. Zaafarany, J.H. Al-Faheem, Y. Abdallah, A.S. Fouda, *Int. J. Electrochem Sci.*,7(8), (2012)6622.
6. F. M. Al- Noisier, M. Abdallah, E.H. El Mossalamy, *Chem Tech Fuels and Oils,* 47(6) (2012) 453.
7. S.S. Abdel-Rahim, K.F. Khaled, N. A. Al-Mubarak , *Arab. J. Chem*., 4(2011) 333.
8. M. El. Faddy, F .Benita, A. Bearish, Y. Karroo, Charafeddine Jamal, B. Lakhrissi, A. Gunboat, I .Ward, A. Zarrouk, *J. Mol. Liq.*, 318(2020) 113973.
9. V. Rajeswari, K Deva Rayan, G. Periasamy V. Periasamy , *J .Surf. Deterg.,* 16 (2013) 571.
10. P. Sangha, D. S. Chauhan, S. S. Chauhan, G.S Ingham, M. A. Qureshi, *J. Mol. Liq.,* 286(2019)110903.
11. Assad Masumi, Moayed Hosseini Sadr , Behead Sultana, *J. Adhes. Sci. Technol.,* 34(2020) 2569.
12. Habib Ashassi- Sorkhabi, Amir Kazempour, Zahra Frusta, *J. Adhes. Sci. Technol., 35* (2021)164.
13. H. Tantawy, K. A. Soliman, H. M. Abd El-Lateef, *J. Clean. Prod*., 250 (2020)119510.
14. M. Abdallah, N. El Guesmi, A. S. Al-Gorier, R. El-Sayed, A. Meshabi, M. Sobhi, *Green Chem. Lett. Rev.* 14 (2021) 381.
15. M. Abdallah, R. El-Sayed, A. Meshabi, M. Alfakeer, *Prot. Met. Phys. Chem. Surf.,* 57 (2021) 389.
16. M. Sobhi, R. El-Sayed, R. M. Abdallah, *J. Surf. Deterg.*,16(2013) 937.
17. R S. Abdel Hameed, E. H Aljuhani, R. Felaly, A. M. Munshi, *J. Adhes. Sci. Technol.,* 36(2020) 27.
18. M. Alfakeer, M. Abdallah, A. Fawzy, *Int. J. Electrochem. Sci.,* 15 (2020) 3283.
19. Arej S Al-Gorair, M. Abdallah, *Int. J. Electrochem. Sci,* 16 (2021) 210771.
20. Jabir H. Al-Fahemia, M. Abdallah, El Shafie A. M. Gad, B.A.AL Jahdaly, *J. Mol. Liq.,* 222(2016)1157.

21. R. S Abdel Hameed, Adam El-Zomrawy, M. Abdallah, S. S. Abed El Rehim, H.I. Al Shafer, Noor Eden Shaher, *Int. J. Corros. Scale Inib.*, 6(2017) 196-208.
22. M. Abdallah, A. Fawzy, H. Hawsawi, *Int. J. Electrochem. Sci.*, 15 (2020) 5650.
23. A. Ali Fathima Sabirneeza , R. Geethanjali, S. Submachine, *Chem. Eng. Comm.*, 202(2015)232.
24. S. A. Umoren, Y. Li, F. H. Wang, *Corros. Sci.*, 52(2010)1777.
25. M. Abdallah, A. Fawzy, H. Hawaii, R.S. Abdel Hameed, SS Al-Quaid, *Int. J. Electrochem. Sci.*, 15(2020)8129.
26. R.S. Abdel Hameed, M.T. Qureshi, M. Abdallah, *Int. J. Corros. Scale Inhib.*, 10 (2021)68.
27. M. Abdallah, M. Alfakeer, Arej S Al-Gorair, A. Al Bahir, M. Sobhi, Int. *J. Electrochem. Sci*, 16 (2021) Article ID: 210622.
28. M. Abdallah, A. Fawzy, M. Alfakeer, *Int. J. Electrochem. Sci.* 15 (2020) 10289-10303.
29. M. Abdallah, Mohamed I. Awed, H.M. Atlas, Moataz Morad, Mona A. Elater, Jabir H Al-Fahmi, Wafaa M. Sayed, *Egypt. J. Pet*., 29(3) (2020)211-218.
30. H. Amar, A. Tounsi, A. Makayssi, A. Derja, J. Benzakour, A. Outzourhit, *Corros.Sci.*,49, (2007) 2936.
31. L. Elkadi, B. Mernari, M. Traisnal, F. Bentiss, M. Lagrenee, *Corros. Sci*.42 (2000) 703.
32. M. Sobhi, M. Abdallah, K. S. Khairou, *Monatsh. Fur Chemie*, 143 (2012)1379.
33. M. Sobhi, R. El-Sayed, M. Abdallah, *Chem. Eng. Comm.*, 203 (2016)758.
34. B. Xu, W. Yang, Y. Liu, X. Yin, W. Gong, Y. Chen, *Corros. Sci*., 78(2014)260.
35. C. H. Hsu, F. Mansfield, *Corrosion*, 57(2001) 747.
36. S. S. Abd El Rehim, M. A. M. Ibrahim, K.F. Khalid, *Mater Chem. Phys.*, 70(2001) 268.
37. O. J Odejobi, E. L. Odekanle, *Results in Mater.*, 5 (2020)100074.
38. O.L. Riggs Jr. and R. M. Hurd, *Corrosion,* 23 (1967) 252.
39. K.J. Laider, Chemical Kinetics, Mc Grew Hill Publishing Company Ltd, 1965.
40. J. Lipkowski, P.N., Ross (Eds.), Adsorption of Molecules at Metal Electrodes, VCH, New York, (1992).
41. Ahmed Fawzy, Metwally Abdallah, Majda Alfakeer, Hatem M. Atlas, Ismail I. Althagafi, Yasser A. El-Ossaily , *Green Chem. Lett. Rev*., 14 (2021) 488.
42. M. Abdallah, E. A.M. Gad, H.M. Altass, Arej S Al-Gorair, Mona A. El-Ere, B.A. Al-Jadedly, Salah S. Al-Juaid, *Desal. Water Treatm.*, 221 (2021) 270.
43. M. Alfakeer, M. Abdallah, R.S. Abdel Hameed, *Prot. Met. Phys. Chem. Surf*., 56 (2020)225.
44. A. Fawzy, I. A. Zaafarany, H. M. Ali, M. Abdallah, *Int. J. Electrochem Sci*., 13 (2018) 4575.
45. Khuram Shahzad, Mostafa H. Sliem, R. A. Shakoor, A. Bhagwat Radian, Ramadan Kahraman, Malik Adeel Umar, Umar Mansour, Aboukir M. Abdullah, *Scientific Reports* **,** 10, (2020)Article number: 4314.
46. Tengshu Chen, Defang Zeng1, Sajin Zhou, *Pol. J. Environ. Stud.* 27 (2018) 1441